NANO LETTERS

2004
Vol. 4, No. 4
643−646

Inelastic Electron Tunneling Spectroscopy of an Alkanedithiol Self-Assembled Monolayer

Wenyong Wang, Takhee Lee, Ilona Kretzschmar, and Mark A. Reed*

Departments of Electrical Engineering, Applied Physics, and Physics, Yale University, P. O. Box 208284, New Haven, Connecticut 06520

Received January 21, 2004; Revised Manuscript Received February 13, 2004

ABSTRACT

Inelastic electron tunneling spectroscopy (IETS) of an alkanedithiol self-assembled monolayer (SAM) is investigated using a nanometer-scale device. The IETS spectrum of the octanedithiol device clearly shows vibrational signatures of an octanedithiolate, $-SC_8H_{16}S-$, bonded to gold electrodes. The pronounced IETS peaks correspond to vibrational modes perpendicular to the junction interface, which include the stretching modes of Au–S (at 33 mV) and C–C (at 133 mV) and the wagging mode of CH_2 (at 158 mV). The observed peak intensities and peak widths are in good agreement with theoretical predictions.

In the past several years, tremendous progress has been made in the electronic transport characterization of self-assembled monolayers (SAMs).[1,2] Alkanethiol ($CH_3(CH_2)_{n-1}SH$) is one molecular system that has been studied extensively because of its ability to form a robust SAM on gold surfaces.[3] Recently, tunneling has been identified as the main conduction mechanism for alkanethiol SAMs formed in a nanometer-scale junction,[4] as expected because the Fermi levels of contacts lie within a large HOMO−LUMO gap (HOMO: highest occupied molecular orbital; LUMO: lowest unoccupied molecular orbital) of a short molecule.[5] In this study, electronic tunneling behavior through alkanethiol SAMs is further investigated with the technique of inelastic electron tunneling spectroscopy (IETS). IETS was developed in the 1960s to study the vibrational spectrum of organic molecules buried inside metal−oxide−metal junctions[6−8] and has since become a powerful spectroscopic tool for molecular identification and chemical bonding investigation.[9] The purpose of our study is to demonstrate that the IETS technique can be utilized for the unique identification of specific molecular species contained in nanometer-scale devices with self-assembled monolayers.

Electronic transport measurements on an octanedithiol SAM were performed using a nanoscale device (Figure 1a)[4] in which a small number of molecules (∼several thousand) are sandwiched between two metallic contacts. This technique provides a stable device structure and makes temperature-variable measurements possible. Details of the device-fabrication process have been reported elsewhere.[4,10] In this study, 150 nm gold is thermally evaporated onto the top of the sample to fill the pore and form one of the metallic contacts. The device is then transferred into a ∼5 mM octanedithiol ($HS(CH_2)_8SH$, denoted as the C8 dithiol, Figure 1b) molecular solution for SAM deposition. The dithiol solution is prepared by adding ∼10 μL of octanedithiol to 10 mL of ethanol. SAM formation is carried out for 24 h inside a nitrogen-filled glovebox with an oxygen level of less than 5 ppm. Then the device is rinsed and transferred to an evaporator, where 200 nm Au is deposited on the opposing side to confine the SAM and form an enclosed device. During the second thermal evaporation step (pressure $\approx 10^{-8}$ Torr), liquid nitrogen flows through the sample holder to reduce thermal damage to the molecular layer.[4] The device is subsequently packaged and loaded into a cryostat for electrical characterizations between 300 and 4.2 K.

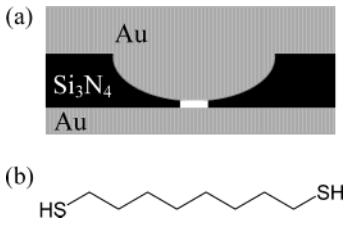

Figure 1. (a) Schematic of the nanopore device. (b) Chemical structure of the C8 dithiol.

Inelastic electron tunneling (IET) spectra are obtained via a standard lock-in second-harmonic measurement technique.[6,11] A synthesized function generator (Stanford Research Systems DS 345) is used to provide both the modulation and the lock-in reference signal. The second-harmonic signal (proportional to d^2I/dV^2) is directly measured using a

* Corresponding author. E-mail: mark.reed@yale.edu.

10.1021/nl049870v CCC: $27.50
Published on Web 03/10/2004

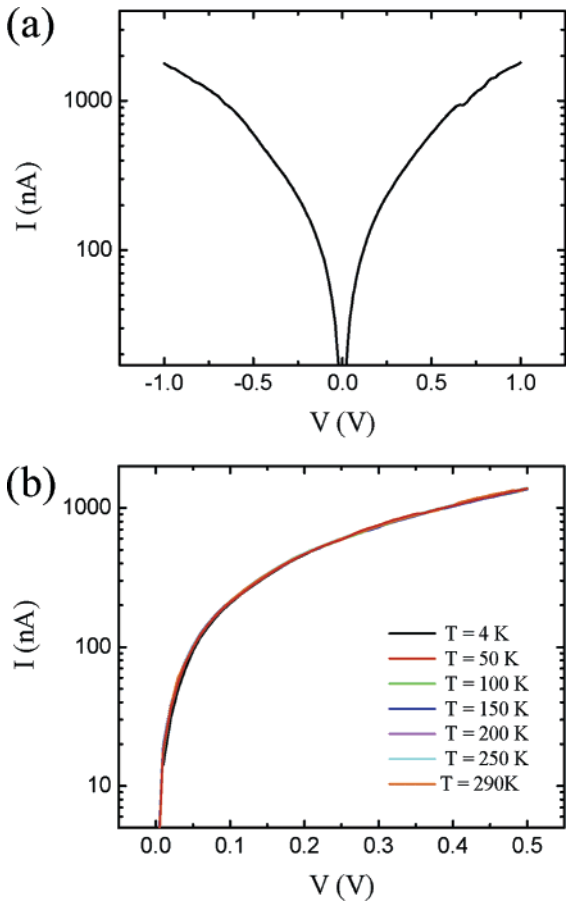

Figure 2. (a) Room-temperature $I(V)$ characteristics of a C8 dithiol SAM. (b) $I(V, T)$ characteristics of the C8 dithiol SAM at selected temperatures (4.2, 50, 100, 150, 200, 250, and 290 K).

lock-in amplifier (Stanford Research Systems 830), which has also been checked to be consistent with a numerical derivative of the first-harmonic signal (proportional to dI/dV). Various modulation amplitudes and frequencies are utilized to obtain the spectra. The ac modulation is added to a dc bias (generated by a Yokogawa 7651 dc source) using operational amplifier-based custom circuitry.[12]

Figure 2a shows a representative current−voltage ($I(V)$) characteristic of a C8 dithiol SAM measured at room temperature using the aforementioned device structure. Positive bias corresponds to electrons injected from the second evaporated Au contact (bottom contact in Figure 1a) into the molecules. Using a junction area of 51 ± 5 nm in diameter (obtained from statistical studies of the nanopore size with a scanning electron microscope), a current density of ∼(9.3 ± 1.8) × 10^4 A/cm^2 at 1.0 V is calculated. Figure 2b shows the temperature-dependent current−voltage ($I(V, T)$) data for this device obtained between 300 and 4.2 K. No significant temperature dependence of the currents is observed between 0 and 0.5 V, confirming that tunneling is the transport mechanism for the C8 dithiol SAM. This result is in agreement with the tunneling transport characteristics observed for alkanemonothiol SAMs.[4]

Figure 3 shows the inelastic electron tunneling spectrum of the same C8 dithiol SAM device obtained at $T = 4.2$ K. An ac modulation of 8.7 mV (rms value) at a frequency of

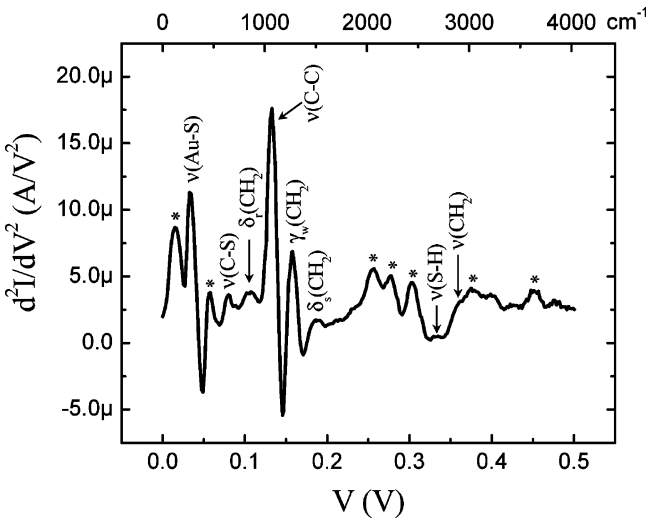

Figure 3. Inelastic electron tunneling spectrum of the C8 dithiol SAM obtained from lock-in second-harmonic measurements with an ac modulation of 8.7 mV (rms value) at a frequency of 503 Hz ($T = 4.2$ K). Peaks labeled * are most probably background due to the encasing Si_3N_4.

Table 1: Summary[a] of the Major Vibrational Modes of Alkanethiolates[b]

modes	methods	wavenumber (cm^{-1})	(meV)
ν(Au−S)	HREELS[14]	225	28
ν(C−S)	Raman[13]	641	79
	Raman[13]	706	88
	HREELS[14]	715	89
δ_r(CH$_2$)	IR[15]	720	89
	IR[15]	766	95
	IR[15]	925	115
	HREELS[14]	1050	130
ν(C−C)	Raman[13]	1064	132
	Raman[13]	1120	139
	IR[15]	1230	152
$\gamma_{w,r}$(CH$_2$)	HREELS[14]	1265	157
	IR[15]	1283	159
	IR[15]	1330	165
δ_s(CH$_2$)	HREELS[14]	1455	180
ν(S−H)	Raman[13]	2575	319
ν_s(CH$_2$)	Raman[13]	2854	354
	HREELS[14]	2860	355
	Raman[13]	2880	357
ν_{as}(CH$_2$)	Raman[13]	2907	360
	HREELS[14]	2925	363

[a] There is a vast amount of literature with spectroscopic assignments for alkanethiols. The references given are representative of IR, Raman, and HREELS assignments. [b] Taken from refs 13−15.

503 Hz was applied to the sample to acquire the second-harmonic signals. The spectra are stable and repeatable upon successive bias sweeps. The spectrum at 4.2 K is characterized by three pronounced peaks in the 0 to 200 mV region at 33, 133, and 158 mV. From comparisons with previously reported infrared (IR), Raman, and high-resolution electron energy loss (HREEL) spectra of SAM-covered gold sur-

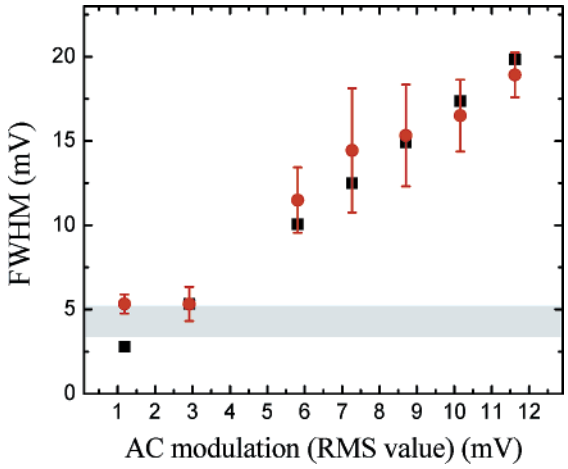

Figure 4. Line broadening of the 133 meV C−C stretching mode as a function of ac modulation at a fixed temperature (4.2 K). The circles are experimental FWHM values, and the squares are theoretical calculations considering both modulation and thermal contributions. The shaded bar denotes the expected saturation due to the derived intrinsic linewidth (including a 5.4kT thermal contribution) of 3.73 ± 0.98 meV.

faces (Table 1), these three peaks are assigned to ν(Au−S), ν(C−C), and $\gamma_w(CH_2)$ modes of a surface-bound alkanethiolate.[13−16] The absence of a strong ν(S−H) signal at ~329 mV suggests that most of the thiol groups have reacted with the gold bottom and top contacts. Peaks are also reproducibly observed at 80, 107, and 186 mV. They correspond to ν-(C−S), $\delta_r(CH_2)$, and $\delta_s(CH_2)$ modes. The stretching mode of the CH_2 groups, $\nu(CH_2)$, appears as a shoulder at 357 meV. The peak at 15 mV is due to vibrations from either Si, Au, or δ(C−C−C).[17] We note that all alkanethiolate peaks without exception or omission occur in the spectra. Peaks at 58, 257, 277, and 302 as well as those above 375 mV are likely to originate from Si−H and N−H vibrations related to the silicon nitride membrane,[17a,18] which forms the SAM encasement. The measurement of the background spectrum of an "empty" nanopore device with only gold contacts to obtain background contributions from Si_3N_4 is hampered by currents that are either too low (open circuit) or too high (short circuit) in such a device. However, to the best of our knowledge alkanethiols have no vibrational signatures in these regions.

Although there are no selection rules in IETS as there are in IR and Raman spectroscopy, certain selection preferences have been established. According to the IETS theory,[19] molecular vibrations with net dipole moments perpendicular to the interface of the tunneling junction have larger peak intensities than vibrations with net dipole moments parallel to the interface (for dipoles close to the electrodes). Thus, vibrations perpendicular to the electrode interface (i.e., ν(Au−S), ν(C−S), ν(C−C), and $\gamma_w(CH_2)$) dominate the IETS spectrum, but modes parallel to the interface (i.e., $\delta_{r,s}(CH_2)$ and $\nu(CH_2)$) are weak.

To verify that the observed spectra are indeed valid IETS data, the peak width broadening was examined as a function of temperature and modulation voltage. IETS was performed with different ac modulations at a fixed temperature and at different temperatures with a fixed ac modulation. Figure 4

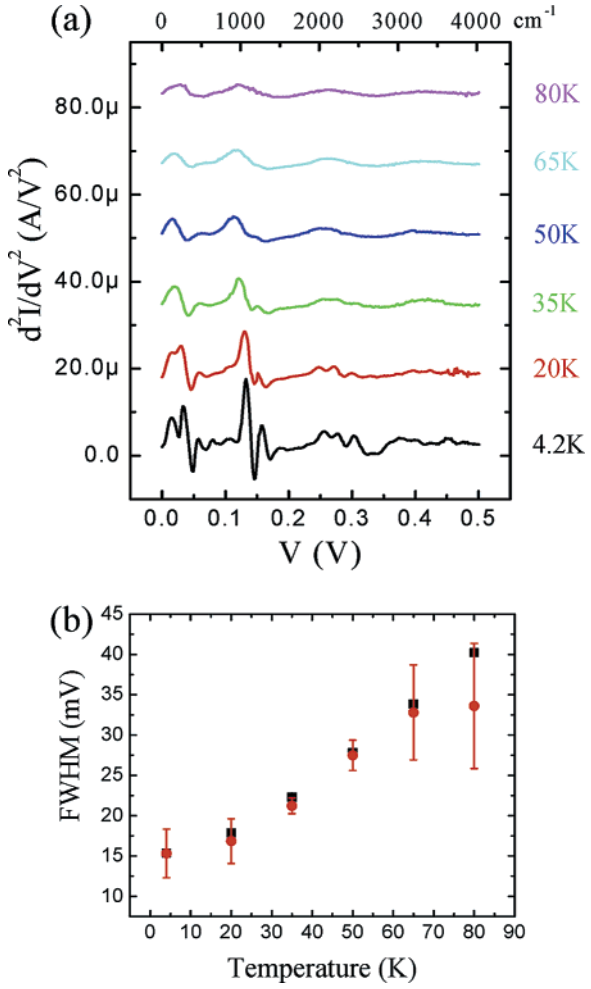

Figure 5. (a) Temperature dependence of IET spectra obtained at a fixed modulation of 8.70 mV (rms value). (b) Line (C−C stretching mode) broadening as a function of temperature. The circles are experimental FWHM values, and the squares are theoretical calculations considering thermal broadening, modulation broadening, and the intrinsic linewidth.

shows the modulation broadening of the C−C stretching mode at 133 meV. The circles are the full widths at half maximum (FWHMs) of the experimental peak at $T = 4.2$ K with various modulation voltages. A Gaussian distribution function was utilized to obtain a FWHM and the error range.[20] The squares are calculated FWHM values ($W_{theoretical}$) taking into account both a finite temperature effect ($W_{thermal} \approx 5.4$ kT)[11] and a finite voltage-modulation effect ($W_{modulation} \approx 1.7\ V_{ac\_rms}$).[21] These two broadening contributions add as the squares: $W^2_{theoretical} = W^2_{thermal} + W^2_{modulation}$. The agreement is excellent over most of the modulation range, but we note a saturation of the linewidth at low modulation voltage, indicating the influence of a nonnegligible intrinsic linewidth. Taking into account the known thermal and modulation broadenings and including the intrinsic linewidth (W_I)[22] broadening as a fitting parameter, the measured peak width (W_{exp}) is given by

$$W_{exp} = \sqrt{W_I^2 + W^2_{thermal} + W^2_{modulation}} \qquad (1)$$

W_I can be determined by using a nonlinear least squares fit

to the ac modulation data (Figure 4) with eq 1, giving an intrinsic linewidth of 3.73 ± 0.98 meV for this line. This is shown (with the error range) in Figure 4 as a shaded bar, including the thermal contribution.

We can independently check the thermal broadening of the linewidth at a fixed modulation. Figure 5a shows the temperature dependence of the IET spectra obtained with an ac modulation of 8.70 mV. In Figure 5b, the circles (and corresponding error bars) are experimental FWHM values of the C−C stretching mode from Figure 5a, determined by a Gaussian fit (and the error of the fit) to the experimental line shape. For simplicity, we have considered only the Gaussian line shapes,[20] resulting in larger error bars for the lower temperature range due to an asymmetric line shape. The squares are theoretical calculations considering thermal broadening, modulation broadening, and the intrinsic linewidth determined above. The error ranges of the calculation (due to the intrinsic linewidth error) are approximately the size of the data points. The agreement between theory and experiment is very good, spanning a temperature range from below ($\times$ 0.5) to above ($\times$ 10) the thermally broadened intrinsic linewidth.

In conclusion, the electronic transport through self-assembled C8 dithiol monolayers was investigated. Tunneling transport was observed as the main conduction mechanism by temperature-independent $I(V)$ characteristics. An inelastic electron tunneling spectroscopy study of a C8 dithiol SAM device exhibited that tunneling charge carriers couple with molecular vibrations. Observed peak intensities and widths of the inelastic tunneling spectra agree well with theoretical predictions.

Acknowledgment. We thank J. F. Klemic, X. Li, and R. Munden for helpful discussions and suggestions. This work was supported by DARPA/ONR (N00014-01-1-0657), ARO (DAAD19-01-1-0592), AFOSR (17496200110358), NSF (DMR-0095215), and NASA (NCC 2-1363). The fabrication was performed in part at the Cornell Nano-Scale Science & Technology Facility. **Note Added in Proof:** This manuscript was submitted simultaneously with a similar result[23] from J. G. Kushmerick et al., reporting IETS on various (including alkanethiol) SAMs. The IETS data of the two manuscripts exhibit both similarities and differences, which reflect the different device geometries and molecules used.

References

(1) *Molecular Nanoelectronics*; Reed, M. A., Lee, T., Eds.; American Scientific Publishers: Stevenson Ranch, CA, 2003.
(2) Nitzan, A.; Ratner, M. A. *Science* **2003**, *300*, 1384.
(3) Ulman, A. *An Introduction to Ultrathin Organic Films from Langmuir−Blodgett to Self-Assembly*; Academic Press: Boston, 1991.
(4) Wang, W.; Lee, T.; Reed, M. A. *Phys. Rev. B* **2003**, *68*, 035416.
(5) Ratner, M. A.; Davis, B.; Kemp, M.; Mujica, V.; Roitberg, A.; Yaliraki, S. *Molecular Electronics: Science and Technology*, Aviram, A., Ratner, M. A., Eds.; Annals of the New York Academy of Sciences; New York Academy of Sciences: New York, 1998; Vol. 852.
(6) Jaklevic, R. C.; Lambe, J. *Phys. Rev. Lett.* **1966**, *17*, 1139.
(7) Adkins, C. J.; Phillips, W. A. *J. Phys. C: Solid State Phys.* **1985**, *18*, 1313.
(8) Hansma, P. K., Ed. *Tunneling Spectroscopy: Capabilities, Applications, and New Techniques*; Plenum: New York, 1982.
(9) Stipe, B. C.; Rezaei, M. A.; Ho, W. *Science* **1998,** *280*, 1732.
(10) Zhou, C.; Deshpande, M. R.; Reed, M. A.; Jones II, L.; Tour, J. M. *Appl. Phys. Lett.* **1997**, *71*, 611.
(11) Lambe, J.; Jaklevic, R. C. *Phys. Rev.* **1968**, *165*, 821.
(12) Horowitz, P.; Hill, W. *The Art of Electronics*; Cambridge University Press: New York, 1989.
(13) For Raman data see, for example, Bryant, M. A.; Pemberton, J. E. *J. Am. Chem. Soc.* **1991**, *113*, 8284.
(14) For HREELS data see, for example, Kato, H. S.; Noh, J.; Hara, M.; Kawai, M. *J. Phys. Chem. B* **2002**, *106*, 9655.
(15) For IR data see, for example, Castiglioni, C.; Gussoni, M.; Zerbi, G. *J. Chem. Phys.* **1991**, *95*, 7144.
(16) The symbols δ, γ, and ν denote in-plane rocking (r) and scissoring (s), out-of-plane wagging (w) and twisting (t), and stretching modes, respectively.
(17) (a) Molinary, M.; Rinnert, H.; Vergnat, M.; Weisbecker, P. *Mater. Sci. Eng., B* **2003**, *69*, 301. (b) Bogdanoff, P. D.; Fultz, B.; Rosenkranz, S. *Phys. Rev. B* **1999**, *60*, 3976. (c) Mazur, U.; Hipps, K. W. *J. Phys. Chem.* **1982**, *86*, 2854.
(18) (a) Mazur, U.; Hipps, K. W. *J. Phys. Chem.* **1981**, *85*, 2244. (b) Kurata, H.; Hirose, M.; Osaka, Y. *Jpn. J. Appl. Phys.* **1981**, *20*, L811.
(19) Kirtley, J.; Hall, J. T. *Phys. Rev. B* **1980**, *22*, 848.
(20) Lauhon, I. J.; Ho, W. *Phys. Rev. B* **1999**, *60*, R8525.
(21) Klein, J.; Léger, A.; Belin, M.; Défourneau, D.; Sangster, M. J. L. *Phys. Rev. B* **1973**, *7*, 2336.
(22) Lauhon, L. J.; Ho, W. *Rev. Sci. Instrum.* **2001**, *72*, 216.
(23) Kushmerick, J. G.; Lazorcik, J.; Patterson, C. H.; Shashidhar, R.; Seferos, D. S.; Bazan, G. C. *Nano Lett.* **2004**, *4*, 639.

NL049870V